Journal of Fluorescence, Vol. 2, No. 4, 1992

Two Photon-Induced Fluorescence Intensity and Anisotropy Decays of Diphenylhexatriene in Solvents and Lipid Bilayers

Joseph R. Lakowicz,[1] Ignacy Gryczynski,[1] Józef Kuśba,[1] and Eva Danielsen[1,2]

Received December 3, 1992; revised February 23, 1993; accepted February 24, 1993

We measured the fluorescence intensity and anisotropy decays of 1,6-diphenyl-1,3,5-hexatriene (DPH)-labeled membranes resulting from simultaneous two-photon excitation of fluorescence. Comparison of these two-photon data with the more usual one-photon measurements revealed that DPH displayed identical intensity decays, anisotropy decays, and order parameters for one- and two-photon excitation. While the anisotropy data are numerically distinct, they can be compared by use of the factor 10/7, which accounts for the two-photon versus one-photon photoselection. The increased time 0 anisotropy of DPH can result in increased resolution of complex anisotropy decays. Global analysis of the one- and two-photon data reveals consistency with a single apparent angle between the absorption and the emission oscillators. The global anisotropy analysis also suggests that, except for the photoselection factor, the anisotropy decays are the same for one- and two-photon excitation. This ideal behavior of DPH as a two-photon absorber, and its high two-photon cross section, makes DPH a potential probe for confocal two-photon microscopy and other systems where it is advantageous to use long-wavelength (680- to 760-nm) excitation.

KEY WORDS: Fluorescence intensity decays; fluorescence anisotropy decays; two-photon excitation; one-photon excitation; diphenylhexatriene; solvents; lipid bilayers.

INTRODUCTION

Two-photon absorption has been of interest to spectroscopists and theoretical chemists because its selection rules are complementary to those governing one-photon absorption [1–4]. Consequently, one can detect electronic transitions which are normally silent in classical absorption spectroscopy. Two-photon absorption spectroscopy has been applied in biophysics for further understanding of polyenes [5], visual pigments [6], and porphyrins [7], and to resolve the ^1L_a and ^1L_b states of indole [8,9].

The absorption due to simultaneous absorption of two-photons is weak, resulting in the frequent use of fluorescence as a means to detect two-photon absorption [10,11]. There have been only a few attempts to use the fluorescence resulting from two-photon excitation to determine properties of biomolecules [12,13]. At present there is a growing interest in the use of the information content of the time-resolved fluorescence resulting from two-photon excitation (TPE).[3] The use of TPE can pro-

[1] University of Maryland School of Medicine, Center for Fluorescence Spectroscopy, Department of Biological Chemistry, 108 North Greene Street, Baltimore, Maryland 21201.

[2] Permanent address: Department of Mathematics and Physics, Royal Veterinary and Agricultural University, Thorvaldsensvej 40, DK-1871 Frederiksberg C, Denmark.

[3] **Abbreviations used:** DPH, 1,6-diphenyl-1,3,5-hexatriene; OPE, one-photon excitation; TPE, two-photon excitation; DPPG, dipalmitoyl-L-α-phosphatidylglycerol; DMPG, dimyristoyl-L-α-phosphatidylglycerol; CHO, cholesterol; POPG, 1-Palmitoyl-2-oleoyl-*sn*-glycero-3-phospho-*rac*-glycerol.

1053-0509/92/1200-0247$06.50/0

vide increased photoselection due to the requirement for simultaneous interactions with two-photons, increase anisotropies at time 0, and increased resolution of anisotropy decays [14]. Additionally, TPE allows intrinsic confocal excitation in fluorescence microscopy, and the use of red or near-infrared excitation can result in decreased autofluorescence and photobleaching of sensitive biochemical samples [15,16]. However, because of the selection rules for one-photon excitation (OPE) and TPE, interpretation of the steady-state and time-resolved spectral parameters is not obvious. For instance, indole [17], proteins [18], and, to a lesser extent, the DNA probe 4′,6-diamidino-2-phenylindole (DAPI) [19] display fundamental (time = 0) anisotropies (r_0) which cannot be accounted for by simple photoselection considerations. To facilitate the use of TPE in studies of biological membranes, we examined the fluorescence spectral properties of 1,6-diphenyl-1,3,5-hexatriene (DPH), which is perhaps the most widely used probe of bilayer order and dynamics [20–23]. We compared the fluorescence intensity and anisotropy decays of DPH in the viscous solvent triacetin and in DPPG, DMPG, or DMPG/CHO bilayers, resulting from OPE and TPE of DPH.

THEORY

Photoselection for One- and Two-Photon Fluorescence Anisotropy

The theory for the anisotropy resulting from OPE and TPE has been described elsewhere in extensive but rather complex reports [24–27]. We describe here only those aspects relevant for our analysis of DPH. Suppose that the absorption and emission oscillators are well described by the oscillating dipole model and that the absorption and emission oscillator form an angle β_i relative to each other, where the subscript 1 or 2 refers to OPE or TPE, respectively. In the absence of rotational motion between absorption and emission, the steady-state anisotropies are given by

$$r_{10}(\beta_1) = \frac{2}{5}\left(\frac{3}{2}\cos^2\beta_1 - \frac{1}{2}\right) \quad (1)$$

$$r_{20}(\beta_2) = \frac{4}{7}\left(\frac{3}{2}\cos^2\beta_2 - \frac{1}{2}\right) \quad (2)$$

The factor 2/5 and 4/7 are the result of the $\cos^2\theta$ and $\cos^4\theta$ dependence of the absorption probabilities of OPE and TPE, respectively, where θ is the angle between the electric field of the incident light and the absorption dipole. The parentheses in Eqs. (1) and (2) refer to the averaging of these absorption probabilities for a randomly oriented sample. Hence, if the transition moments for OPE and TPE display the same apparent angle, i.e., $\beta_1 = \beta_2$, and the anisotropies display the ratio

$$\frac{r_{20}}{r_{10}} = 10/7 = 1.429 \quad (3)$$

In the case of a time-resolved decay this ratio at times greater than zero can be expected to persist throughout the decay, assuming that OPE and TPE result in an excited state with the same orientation within the molecular framework. Such a constant ratio was observed for benzene in the absence of rotational diffusion [27]. If the absorption and emission transitions are parallel, i.e., $\beta_1 = \beta_2 = 0$, then $r_{10} = 0.40$ and $r_{20} = 0.57$ [14].

MATERIALS AND METHODS

Frequency-domain measurements for OPE and TPE were performed using a 10-GHz frequency-domain fluorometer described elsewhere in detail [28,29]. For two-photon excitation we used the fundamental output from a cavity-dumped pyridine2 dye laser, which was synchronously pumped by a mode-locked argon ion laser. The pulse repetition rate of dye laser was 3.975 MHz and the half-width of the pulse was near 6 ps. The detection was provided by a high-speed microchannel plate photomultiplier tube (R2566U Hamamatsu, 6-μ channels) which is essentially free of color effect. All measurements used scattered light as the reference, except for 716-nm excitation, where DMSS (4-diethylamine-ω-methylsulfonyl-*trans*-styrene) was used with a reference lifetime of 34 ps [48]. The excitation beam was focused using a 5-cm-focal length lens. A similar lens was used for the collection of the fluorescence. For the one-photon experiments we used 0.5 × 0.5-cm cuvettes with excitation and emission near a corner of the cuvette positioned at the center of a 1 × 1-cm cuvette holder. For the two-photon experiments we used 1.0 × 0.5-cm cuvettes with the long axis aligned with the incident light and with the focal point positioned about 0.5 cm from the surface facing the incident light. The position of the cuvette was adjusted so that the excitation laser beam crossed the solution near the observation window. For OPE, we used the frequency-doubled output of the same dye laser. The emission intensity as a function of exci-

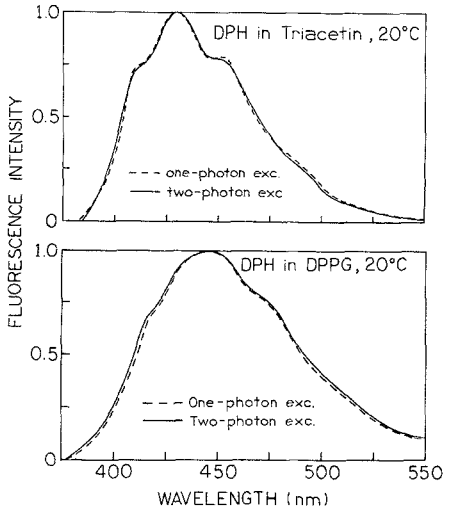

Fig. 1. Fluorescence emission spectra of DPH in triacetin (top) and in DPPG bilayers (bottom) for excitation at 358 nm (---) and 716 nm (—).

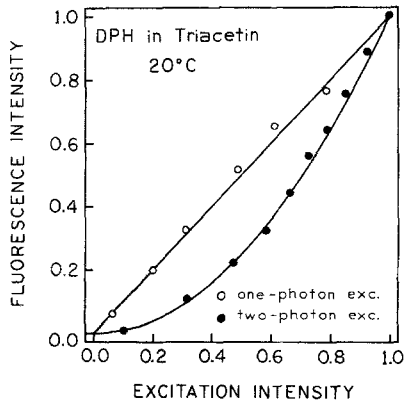

Fig. 2. Dependence of the DPH emission intensity on the excitation intensity at 358 (○) and 716 nm (●). The intensities were normalized to unity at the highest excitation intensities. The solid lines represent linear and quadratic curves and are not fitted curves.

tation intensity was measured by attenuating the light with neutral-density filters. Transmission of the filters at the relevant wavelength were measured in a conventional spectrophotometer.

Emission spectra were obtained using a monochromator with a bandpass of 10 nm. The time-resolved and limiting anisotropy values were measured without the monochromator using glass cutoff filters, Corning 3-74 and 4-96. Emission spectra and frequency-domain intensity decays were measured under "magic angle" conditions. Unless otherwise indicated, the excitation was at 358 and 716 nm for OPE and TPE, respectively.

To allow comparison of the OPE and TPE data, the same solutions were used for both types of experiments. In triacetin the concentration of DPH was 10^{-4} *M*. Lipid vessels were prepared by sonification in 20 m*M* Tris, pH = 8, at a final lipid concentration near 5 m*M*. DPH was added as a solution in tetrahydrofuron, to a final concentration of 5×10^{-5} *M*, yielding a 100:1 lipid:DPH ratio. These relatively high concentrations were chosen to minimize the ratio of background to signal and to maximize the weak signal from two-photon excitation. The samples of triacetin or lipids, without DPH, did not display significant signals (<1%) under our experimental conditions.

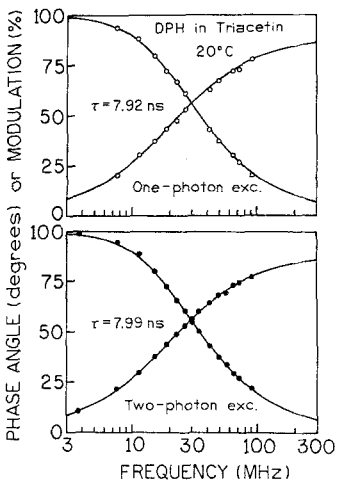

Fig. 3. Frequency-domain intensity decay of DPH in triacetin observed for OPE at 358 nm (top) and TPE at 716 nm (bottom).

Frequency-Domain Intensity and Anisotropy Decay Analysis

The intensity decays were recovered from the frequency-domain data in terms of the multiexponential model

$$I(t) = \sum_i \alpha_i e^{-t/\tau_i} \tag{4}$$

The values of α_i and τ_i are obtained by comparison of the experimental phase (φ_ω) and modulation (m_ω) values, with calculated (subscript c) values, as given by the

$$\chi_R^2 = \frac{1}{\nu} \sum_\omega \left[\frac{\varphi_\omega - \varphi_{\omega c}}{\delta\varphi} \right]^2 + \frac{1}{\nu} \sum_\omega \left[\frac{m_\omega - m_{\omega c}}{\delta m} \right]^2 \tag{5}$$

ω is the light modulation frequency in radians per second [30,31], and ν is the number of degrees of freedom. In our case ν is given by two times the number of modulation frequencies minus the number of variable parameters.

Table I. Anisotropy Decay Parameters of DPH in Triacetin[a]

	One-photon Excitation				Two-photon excitation			
°C	τ (ns)	θ (ns)	r_{10}	χ_R^2	τ (ns)	θ (ns)	r_{20}	χ_R^2
10	8.04	3.92 (3.80–4.04)[b]	0.372 (0.370–0.374)	0.74	8.29	3.89 (3.82–3.97)	0.522 (0.519–0.525)	0.98
20	7.92	1.99 (1.95–2.03)			7.99	1.88 (1.84–1.93)		
30	7.54	1.06 (1.03–1.08)			7.60	1.07 (1.05–1.10)		
40	7.27	0.66 (0.64–0.69)			7.21	0.62 (0.61–0.63)		

[a]Limited anisotropies (r_{10} and r_{20}) were global parameters and correlation times (θ) were nonglobal parameters. The lifetimes (τ) were measured separately using "magic angle" conditions and found to be single exponentials in this solvent.

[b]Confidence intervals obtained from the least-squares analysis [43,44].

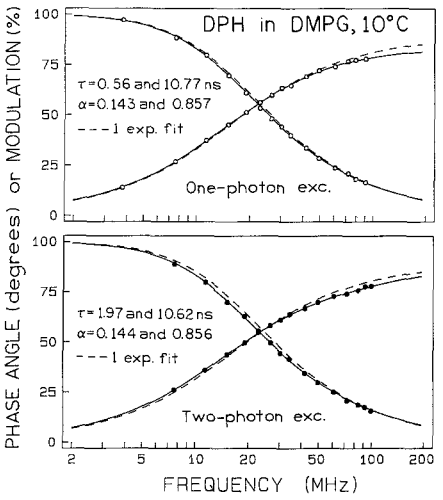

Fig. 4. Frequency-domain intensity decay for DPH in DMPG vesicles, 10°C, for OPE at 358 nm (top) and TPE at 716 nm (bottom).

The anisotropy decays were also analyzed as a multiexponential decay,

$$r_k(t) = \sum_j r_{k0} g_j e^{-t/\theta_j} \tag{6}$$

where θ_j is the individual correlation time, g_j the fractional amplitude associated with the jth correlation time, and r_{k0} the fundamental (time 0) anisotropy for OPE (r_{10}) and TPE (r_{20}). This equation assumes that g_j and θ_j do not depend on the mode of excitation, which is consistent with our experimental results. To avoid the use of three subscripts on r, we chose to represent the amplitude of the anisotropy decay associated with the jth decay time as $r_{k0}g_j$. One expects $r_{k0} = r_{k0} \Sigma g_j$, where $\Sigma g_j = 1$. That is, r_{k0} is the time 0 anisotropy for OPE ($k = 1$) or TPE ($k = 2$), and g_j represents the fraction of the anisotropy which decays with the jth correlation time.

In the frequency domain we observe two quantities which characterize the anisotropy decay. These are the phase shift Δ_ω between the perpendicular ($\phi_\perp$) and parallel ($\phi_\parallel$) components of the emission,

$$\Delta_\omega = \varphi_\perp - \varphi_\parallel \tag{7}$$

and the ratio

$$\Lambda_\omega = \frac{m_\parallel}{m_\perp} \tag{8}$$

of the parallel ($m_\parallel$) and the perpendicular ($m_\perp$) components of the modulated emission. For graphical presentation we use the frequency-dependent anisotropy (r_ω), which is defined by

$$r_\omega = \frac{\Lambda_\omega - 1}{\Lambda_\omega + 2} \tag{9}$$

The parameters describing the anisotropy decay are obtained by minimizing the squared deviations between measured and calculated values, using

$$\chi_R^2 = \frac{1}{\nu} \sum_{\omega,k} \left[\frac{\Delta_\omega - \Delta_{\omega c}}{\delta\Delta} \right]^2 + \frac{1}{\nu} \sum_{\omega,k} \left[\frac{\Lambda_\omega - \Lambda_{\omega c}}{\delta\Lambda} \right]^2 \tag{10}$$

where $\delta\Delta$ and $\delta\Lambda$ are the uncertainties in the differential phase and modulation ratio, respectively [32,33], and k indicates OPE and/or TPE (below). The use of both one- and two-photon data in the analysis corresponds to a global analysis of these data.

Table II. Multiexponential Analysis of DPH Intensity Decays in Lipids

			One-photon excitation				Two-photon excitation			
Lipid	°C	n	τ_i (ns)	α_i	f_i	χ^2_R	τ_i (ns)	α_i	f_i	χ^2_R
DPPG	20	1	8.99	1.0	1.0	18.1	8.65	1.0	1.0	18.7
		2	4.45	0.202	0.101		3.95	0.177	0.081	
			10.09	0.798	0.899	2.9	9.65	0.823	0.919	2.2
						(9.9)[a]				(9.8)[b]
	55	1	7.34	1.0	1.0	3.9	7.10	1.0	1.0	18.0
		2	5.86	0.411	0.329		2.87	0.150	0.061	
			8.35	0.589	0.671	1.8	7.73	0.850	0.939	2.9
						(16.2)				(16.7)
POPG	10	1	9.03	1.0	1.0	11.8	8.77	1.0	1.0	31.6
		2	1.94	0.078	0.017		3.36	0.187	0.072	
			9.43	0.922	0.983	1.9	9.85	0.813	0.928	2.8
						(13.4)				(16.7)
	40	1	7.57	1.0	1.0	17.5	7.43	1.0	1.0	28.8
			1.19	0.102	0.017		1.78	0.131	0.033	
			7.93	0.898	0.983	2.0	8.01	0.869	0.967	2.5
						(5.0)				(5.6)
DMPG	10	1	10.38	1.0	1.0	9.5	9.86	1.0	1.0	44.1
		2	0.54	0.154	0.009		1.95	0.139	0.029	
			10.76	0.846	0.991	1.8	10.69	0.861	0.971	1.7
						(9.9)[a]				(21.8)[b]
	40	1	8.39	1.0	1.0	1.8	8.40	1.0	1.0	4.2
		2	7.33	0.206	0.180		8.01	0.903	0.858	
			8.66	0.794	0.820	1.7	12.34	0.097	0.142	2.5
						(2.7)				(2.8)
DMPG/CHO	10	1	10.58	1.0	1.0	3.3	9.95	1.0	1.0	26.8
		2	0.07	0.232	0.002		1.65	0.105	0.019	
			10.67	0.778	0.998	2.7	10.51	0.895	0.482	2.1
						(19.2)				(20.3)
	40	1	9.98	1.0	1.0	2.8	9.69	1.0	1.0	14.7
		2	5.50	0.072	0.040		4.27	0.150	0.066	
			10.31	0.928	0.960	2.1	10.59	0.850	0.934	2.7
						(12.3)				(14.5)

[a]From cross fits of the OPE data to the two-photon intensity decay parameters.
[b]From cross fits of the TPE data to the one-photon intensity decay parameters.

Global Analysis of Anisotropy decays for OPE and TPE

The fundamental anisotropies are related to the angle β between the absorption and the emission dipoles [Eqs. (1) and (2)]. One can test whether the one- and two-photon data are consistent with a single value of β by analyzing the anisotropy decays in terms of β-dependent amplitudes. For global analysis of one- and two-photon anisotropy decays, we assumed that the correlation times (θ_j), fractional amplitude (g_j), and β values were the same for OPE and TPE. Hence,

$$r_1(t) = r_{10}(\beta) \sum_j g_j e^{-t/\theta_j} \quad (11)$$

$$r_2(t) = r_{20}(\beta) \sum_j g_j e^{-t/\theta_j} \quad (12)$$

and the goodness of fit is given by Eq. (10), where the sum extends over both $k = 1$ and $k = 2$. The expression for the frequency-domain anisotropy and its extension to a multiexponential intensity decay are given in the Appendix.

Interpretation of Limiting Anisotropies in Terms of Cone Angles and Order Parameters

The anisotropy decays of DPH often display nonzero anisotropies at times long compared to the fluorescence lifetime. For a single-correlation time (θ) case, a hindered anisotropy decay is then described by

$$r_k(t) = (r_{k0} - r_{k\infty})e^{-t/\theta} + r_{k\infty} \quad (13)$$

where $r_{k\infty}$ is the long-time anisotropy. If the analysis is

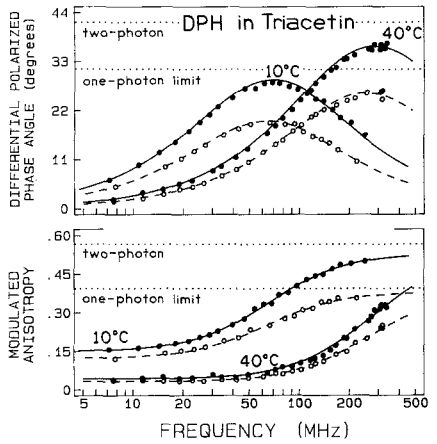

Fig. 5. Frequency-domain anisotropy decay data for DPH in triacetin obtained with OPE (○) and TPE (●). The horizontal dotted lines indicate maximal values of differential phases (upper panel) and modulated anisotropies (lower panel) for one- and two-photon excitation.

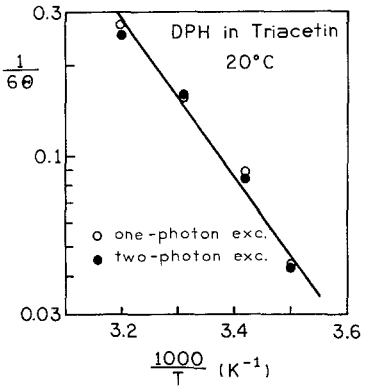

Fig. 6. Arrhenius dependence of the rotational rates [$R = 1/(6\theta)$] of DPH in triacetin obtained with OPE (○) and TPE (●).

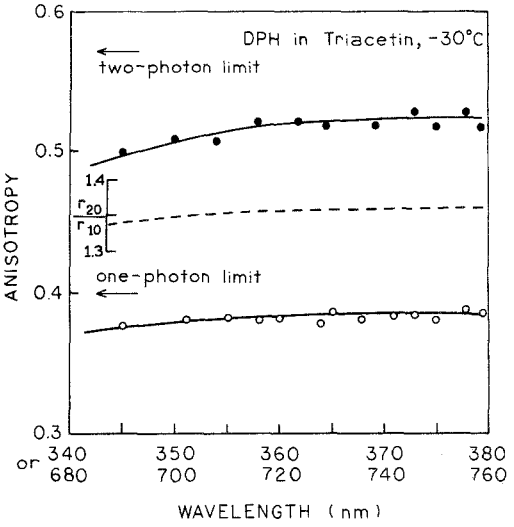

Fig. 7. Steady-state anisotropy spectrum of DPH in triacetin at −30°C obtained with OPE (○) and TPE (●).

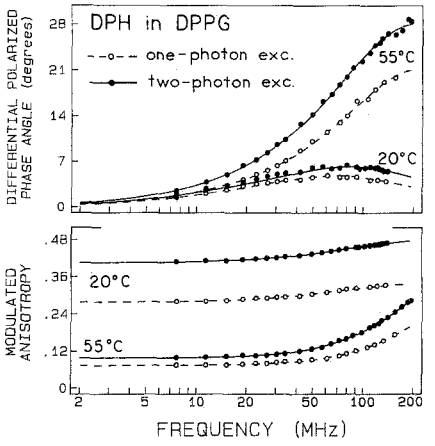

Fig. 8. Frequency-domain anisotropy decay data for DPH in DPPG obtained with OPE (--○--) and TPE (—●—).

performed using two correlation times [$j = 2$ in Eq. (6)], then the amplitude associated with the long-time anisotropy can be used as $r_{k\infty}$. The values of $r_{1\infty}$ from OPE have been used previously to estimate the order parameters (S) of membranes [23]

$$s_1^2 = \frac{r_{1\infty}}{r_{10}} \tag{14}$$

Hence we used the analogous expression $S_2^2 = (r_{2\infty}/r_{20})$ to estimate the order parameter from the two-photon data.

The limiting anisotropies can also be used to estimate the angular displacement of the probe molecule. The model of Kawato *et al.* [22] interprets $r_{1\infty}$ in terms of the angle (θ_c) beyond which the probe (DPH) cannot rotate within the bilayers. We assume that analogous expressions are correct of OPE ($k=1$) and TPE ($k=2$). Hence,

$$\frac{r_{k\infty}}{r_{k0}} = \left[\frac{1}{2}\cos\theta_{kc}(1 + \cos\theta_{kc})\right]^2 \tag{15}$$

An alternative interpretation of $r_{k\infty}$ relates its value to the ensemble average value of the cos θ_{ka}

$$\frac{r_{k\infty}}{r_{k0}} = \left(\frac{3\cos^2\theta_{ka} - 1}{2}\right)^2 \tag{16}$$

Maximal Observable Differential Polarized Phase Angle

For an isotropic rotator [i.e., one correlation time in Eq. (6)], the maximum observable phase angle, at a

Table III. Anisotropy Decay Parameters for DPH in Fluorescence in Lipids

			One-photon excitation			Two-photon excitation		
Lipid	T (°C)	Model[a]	θ_i (ns)	$r_{10}g_j$	χ^2_R	θ_i (ns)	$r_{20}g_j$	χ^2_R
DPPG	20	1 θ	37.13	0.323	96.2	35.74	0.461	270.0
		θ, r_∞	3.42	0.089		2.82	0.102	
			⟨∞⟩[b]	0.256	1.9	⟨∞⟩	0.385	4.1
		2 θ	2.96	0.081		2.37	0.093	
			313.01	0.265	1.3	297.11	0.397	1.8
	55	1 θ	1.54	0.265	126.5	1.32	0.409	160.1
		θ, r_∞	0.83	0.309		0.80	0.427	
			⟨∞⟩	0.044	1.6	⟨∞⟩	0.051	2.6
		2 θ	0.80	0.311		0.89	0.426	
			83.09	0.047	1.3	88.84	0.053	2.4
POPG	10	1 θ	8.58	0.317	108.4	8.86	0.442	256.6
		θ, r_∞	4.17	0.235		4.18	0.332	
			⟨∞⟩	0.105	3.93	⟨∞⟩	0.148	1.2
		2 θ	3.47	0.202		3.93	0.317	
			49.0	0.142	1.1	138.3	0.165	1.1
POPG	40	10	3.82	0.262	136.7	3.19	0.392	264.9
		θ, r_∞	1.68	4.17		1.62	0.332	
				⟨∞⟩	2.1	⟨∞⟩	0.082	2.0
		2 θ	1.57	0.262		1.62	0.403	
			82.20	0.074	1.5	166.4	0.080	1.1
DMPG	10	1 θ	64.60	0.358	76.1	62.29	0.513	273.2
		θ, r_∞	4.34	0.071		4.45	0.101	
			⟨∞⟩	0.304	2.3	⟨∞⟩	0.435	2.4
		2 θ	4.38	0.070		4.18	0.097	
			740.91	0.304	2.2	1288.0	0.440	2.2
	40	1 θ	2.13	0.295	253.6	2.63	0.382	498.1
		θ, r_∞	1.13	0.298		1.13	0.435	
			⟨∞⟩	0.065	2.3	135.13	0.092	2.5
		2 θ	1.10	0.297		1.10	0.435	
			153.17	0.068	2.0	135.13	0.097	1.8
DMPG/CHO	10	1 θ	90.63	0.344	39.7	99.82	0.489	134.3
		θ, r_∞	3.96	0.050		3.71	0.065	
			⟨∞⟩	0.307	3.9	⟨∞⟩	0.443	3.8
		2 θ	3.06	0.043		3.32	0.061	
			468.22	0.316	3.5	1291.0	0.448	3.7
	40	1 θ	30.2	0.279	329.2	38.54	0.389	624.1
		θ, r_∞	1.20	0.133		1.28	0.171	
			⟨∞⟩	0.226	3.0	⟨∞⟩	0.326	2.3
		2 θ	1.18	0.133		1.29	0.170	
			493.4	0.229	2.4	1256.4	0.325	2.2

[a] 1 θ, single-correlation time fit with a floating value of r_{k0}; θ, r_∞, single-correlation time fit with a floating value of r_∞; 2 θ, two-correlation time fit with $r_\infty = 0$.

[b] This analysis corresponds to the "hindered rotation" model, which is similar to a two-correlation time model in which one rotational correlation time is infinity.

given modulation frequency, is independent of the correlation time and is given by

$$\tan \Delta_{max} = \frac{3\omega\tau r_{k0}}{(2 + r_{k0}) + 2[m_{k0}(1 + \omega^2\tau^2)]^{1/2}} \quad (17)$$

where $m_{k0} = (1 + 2r_0)(1 - r_{k0})$ and the intensity decay [Eq. (1)] is assumed to be a single exponential with a decay time τ. This expression displays a high frequency (ω) limit which is independent of ω or τ [35],

$$\tan \Delta_{k0} = \frac{3r_{k0}}{2[(1 + 2r_{k0})(1 - r_{k0})]^{1/2}} \quad (18)$$

In this expression the subscript 0 refers to a limiting value, analogous to the definition of r_0, and the subscript $k = 1$ or 2 refers to one-photon or two-photon excitation, respectively. For one-photon excitation and coli-

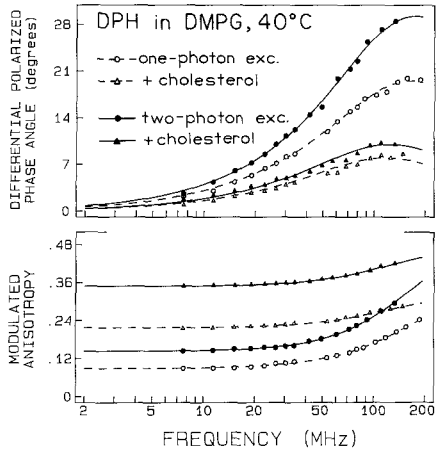

Fig. 9. Frequency-domain anisotropy decay data for DPH in DMPG at 40°C in the presence and absence of cholesterol obtained using OPE (△, ○) and TPE (▲, ●).

near absorption and emission dipoles, $r_{10} = 0.4$ and the maximal value of Δ is $\Delta_{10} = 30°$. For two-photon excitation r_{20} can be as high as 0.57, resulting in a maximal value of $\Delta_{20} = 41.8°$. Observation of Δ values larger than 30° can be considered to be proof of two-photon excitation.

RESULTS AND DISCUSSION

Emission Spectra and DPH Intensity Decays for OPE and TPE

Emission spectra of DPH in triacetin and DPPG bilayers are shown in Fig. 1. The emission spectra resulting from OPE and TPE are superimposable, demonstrating that emission occurs from the same excited state independent of the mode of the excitation. The fact that the emission is due to a biphotonic process is demonstrated in Fig. 2, which shows a quadratic dependence of the DPH emission intensity on the excitation at 716 nm but a linear dependence on the intensity at 358 nm. It should be noted that observation of identical emission spectra for one- and two-photon excitation was not an obvious result. It is known that there are lower energy states of polyenes such as DPH and diphenyloctatetraene which can be reached by TPE [36,37]. Additionally, a recent report suggested the presence of emission from

Table IV. Global Analysis of DPH Fluorescence Anisotropy Decays Obtained with OPE and TPE

Lipid/solvent	T (°C)	θ_1 (ns)	θ_2 (ns)	β (deg)	g_2	$r_{10}{}^a$	$r_{20}{}^a$	χ^2_R
DPPG	20	2.45	262.3	17.9	0.807	0.343	0.490	6.9
		2.98	⟨∞⟩[b]	18.3	0.782	0.341	0.487	8.9
	55	0.88	110.5	18.5	0.116	0.340	0.485	3.8
		0.89	⟨∞⟩	18.8	0.112	0.338	0.483	3.9
POPG	10	3.75	86.9	18.4	0.365	0.340	0.486	3.0
		4.15	⟨∞⟩	18.8	0.309	0.338	0.482	4.2
	40	1.58	104.8	18.6	0.187	0.339	0.484	2.8
		1.65	⟨∞⟩	19.1	0.173	0.335	0.479	3.2
DMPG	10	4.23	1709.9	11.6	0.818	0.376	0.537	2.2
		4.43	⟨∞⟩	11.7	0.811	0.375	0.536	2.3
	40	1.11	133.5	13.4	0.184	0.368	0.525	2.5
		1.14	⟨∞⟩	14.0	0.177	0.365	0.521	3.0
DMPG/CHO	10	3.19	843.6	15.6	0.881	0.357	0.510	4.9
		3.75	⟨∞⟩	15.8	0.870	0.356	0.508	4.5
	40	1.24	3471.6	16.4	0.646	0.352	0.503	4.0
		1.23	⟨∞⟩	16.3	0.645	0.354	0.503	4.0
Triacetin	10	3.90	—	13.4	—	0.368	0.526	0.8[c]
	20	1.96	—	13.5	—	0.367	0.525	1.2
	30	1.08	—	13.9	—	0.365	0.522	0.6
	40	0.61	—	13.0	—	0.369	0.528	0.8

[a]Derived parameters.

[b]This analysis corresponds to the "hindered rotator" model, which is similar to a two-correlation time model in which one rotational correlation time is infinity.

[c]In triacetin the measurements include high-frequency data, where the values of $\delta\Delta$ and $\delta\Lambda$ are larger and were derived from the experimental data. The range of $\delta\Delta$ values was from -0.5 to $+0.5°$, and that of the $\delta\Lambda$ values was from -0.01 to $+0.01°$.

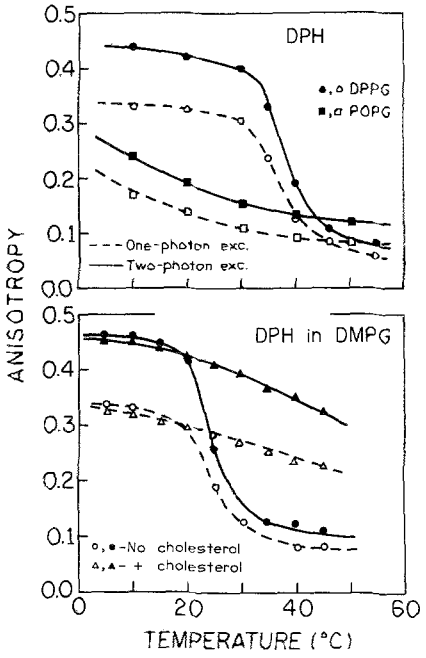

Fig. 10. Temperature dependencies of steady-state anisotropies of DPH in lipids. Top: DPH in DPPG or POPG. Bottom: DPH in DMPG in the absence and presence of cholesterol. The open symbols and dashed lines refer to OPE, and filled symbols and solid lines to TPE.

ground-state cis conformers of DPH [38]. It is possible that TPE could have resulted in selective excitation of such conformers, resulting in an increased contribution of these conformers to the observed emission. We note that the two-photon emission spectra in Fig. 1 were not collected over a range of excitation wavelength, or with adequate precision, to detect the modest spectral shifts expected for cis-conformer emission [38]. Exclusion of the emission of cis-conformers requires additional experimentation and analysis.

Frequency-domain intensity decays of DPH in triacetin at 20°C are shown in Fig. 3. The intensity decays for OPE and TPH are both single exponentials and display the same decay time independent of the mode of excitation. Similarly identical single-exponential decays for OPE and TPE were observed from 10 to 40°C (Table I). The intensity decays of DPH in lipid were found to be multiexponential (Fig. 4 and Table II), as has been observed previously by other time- or frequency-domain measurements using one-photon excitation [20]. In the case of membrane-bound DPH, several authors have proposed that the minor components in the intensity decay are due to a subpopulation of DPH which is in unusual conformations and/or environments [39,40]. If these populations are selectively excited to a different extent for one- and two-photon excitation, then the amplitudes (α_i) of the intensity decay are expected to depend on the mode of excitation. However, the α_i and τ_i values are practically unchanged for OPE and TPE. The similarity of the DPH intensity decays for OPE and TPE is illustrated in Fig. 4 for DPH in DMPG at 10°C. Additional multiexponential intensity decays are given in Table II, for DPPG, DMPG, and DMPG/CHO, at 10 to 55°C. While the precise α_i and τ_i values are not identical in every case, the frequency responses for OPE and TPE are similar (not shown). Fitting the one-photon data to

Table V. Order Parameters of Lipid Bilayers with DPH Obtained upon One- and Two-Photon Excitation

Lipid	T (°C)	r_{20}/r_{10}	$r_{1\infty}/r_{2\infty}$	S_1^2	S_2^2	θ_{1c}	θ_{2c}	θ_{1a}	θ_{2a}
DPPG	20	1.416[a]	1.504[b]	0.742[c]	0.790[c]	25.3[d]	22.5[d]	17.7[e]	15.8[e]
	55	1.338	1.159	0.125	0.107	61.4	63.2	41.0	42.1
POPG	10	1.401	1.412	0.309	0.308	48.1	48.2	32.9	33.0
	40	1.438	1.468	0.199	0.169	55.2	57.7	37.4	38.8
DMPG	10	1.436	1.431	0.811	0.812	21.2	21.1	14.9	14.9
	40	1.457	1.415	0.179	0.175	56.7	57.1	38.3	38.5
DMPG/CHO	10	1.418	1.443	0.860	0.872	18.0	17.2	12.7	12.1
	40	1.367	1.442	0.630	0.656	31.2	30.6	21.8	20.9

[a]Obtained from the best two-correlation time (Table III) assuming $r_{ko} = \Sigma\, r_{k\infty} g_i$. The ratio of limited anisotropies with two- and one-photon excitation is expected to be 1.429 = (4/7)/(2/5) for colinear oscillators (see Theory).

[b]Obtained from "hindered rotator model" [Eq. (13), Table III].

[c]$S_k^2 = r_{k\infty}/r_{ko}$, $r_{k\infty}$, and $r_{k\infty}$ are from the hindered rotator model (Table III), where $k = 1$ or 2 refers to one- or two-photon excitation, respectively. Essentially the same values were obtained from the two-correlation time model.

[d]Calculated from Kinosita *et al* [22], Eq. (15), as degrees.

[e]Calculated from Eq. (16), as degrees.

the best two-photon parameters, and vice versa, resulted in a modest increases in χ^2_R (Table II). We do not feel that these χ^2_R increases indicate a significantly different decay law for DPH for OPE and TPE, but rather the major portion of the χ^2_R increase is due to the slightly shorted lifetime of DPH for TPE. Clarification of this small effect requires additional experimentation and analysis.

Anisotropy Decays of DPH for OPE and TPE

We questioned whether DPH displayed the same correlation times for one- and two-photon excitation. While DPH typically displays a single correlation time for OPE in homogeneous solution, this is not because DPH is an isotopic rotator but, rather, because the absorption and emission dipoles are oriented along the long axis of the molecule. Hence, only the slower motions which displace the longer axis are active in depolarization. The faster motions around the long axis do not displace the transition moments and do not result in decreased anisotropies.

Frequency-domain anisotropy data for DPH in the viscous solvent triacetin are shown in Fig. 5. The time 0 anisotropies (r_0) and correlation times are summarized in Table I. Evidently, DPH displays the same correlation times for one- and two-photon excitation. The r_0 values display a ratio of 1.40, very near the expected values for colinear transitions for OPE and TPE. The correlation times for OPE and TPE display the same Arrehenius dependence (Fig. 6), and in the absence of rotation (-30°C), the r_0 values display a constant ratio of about 1.35 from 340 (680 nm) to 380 (760 nm) (Fig. 7). DPH in triacetin at 40°C displays differential phase angles in excess of 30° (Fig. 5), which demonstrate that there is increased photoselection above what is possible for single-photon excitation [Eq. (18)].

Anisotropy Decay of DPH in Bilayers

Frequency-domain anisotropy data for DPH are shown in Fig. 8 for the DPPG bilayer. These data are characteristic of DPH-labeled bilayers. The decrease in the differential phase angles at 20°C below the lipid phase transition is due primarily to the hindered motion of DPH [41,42]. The larger values of Δ_ω and r_ω are the result of increased orientation of the photoselected population for TPE. The parallel nature of the frequency-domain data for OPE and TPE suggests that the anisotropy decays are similar at all times, except for the amplitude factor.

Anisotropy decays were determined for several lipid bilayers at selected temperature above and below the phase transitions (Table III). Typical results for DMPG with and without cholesterol are shown in Fig. 9. The data could not be fit to a single correlation time with $r_\infty = 0$ (1θ model in Table III) but were well fit by the hindered rotator model [θ, r_∞; Eq. (13)]. The fits were only slightly improved by allowing two correlation times (2θ model), and one of the correlation times is long. Importantly, essentially the same correlation times and amplitudes were observed for OPE and TPE. This demonstrates that, except for the OPE-to-TPE anisotropy ratio, the anisotropy decays of DPH are the same as in the lipid bilayers over a wide range of temperatures and lipid composition.

A more rigorous test of the similarity of the one- and two-photon anisotropy decays is given in Table IV, where we performed a global fit to the data assuming the same values of β_k, θ_j, and g_j for one- and two-photon excitation. For the solvent triacetin and DPPG bilayer the χ^2_R values remain acceptable for global analysis of the one- and two-photon data. Similarly, the χ^2_R values for the global anisotropy analysis of DPH in bilayer are also acceptable. The ability to fit the OPE and TPE anisotropy data globally to the same parameters provides convincing evidence for the similarity of the DPH anisotropy decays induced by OPE or TPE. This point is supported by Fig. 10, which shows the steady-state anisotropies of DPH-labeled bilayers. It is clear that the anisotropy values for OPE and TPE are similar, except for the increased photoselection resulting from TPE. A plot of the ratios r_{20}/r_{10} for these lipids over the standard temperature range reveals values consistently over 1.3 (not shown). The precise values vary for 1.31 to 1.41 depending on lipid, but in all cases the ratios are independent of temperature, which probably indicates small systematic differences between the experiments.

The anisotropy decays (Table IV) were used to calculate the bilayer order parameters (Table V). These results show that essentially the same order parameters and cone angles were obtained for OPE and TPE. This suggests that DPH can be used in a wide variety of one- and two-photon experiments and can be assumed to yield the same information independent of the mode of excitation.

APPENDIX

Analysis of Frequency-Domain Anisotropy Decays with a Multiexponential Intensity Decay

Suppose that the intensity and anisotropy decays are given by Eqs. (4) and (6), respectively, and that the

components in each decay are nonassociated [45–47]. This means that all the individual components in both decays are due to a single population of emitting molecules, each of which displays a multiexponential intensity and anisotropy decay. For such a system the parallel ($\|$) and perpendicular ($\perp$) components of the emission are given by

$$I_{\|}(t) = \frac{1}{3}I(t)[1 + 2r(t)] \tag{A1}$$

$$I_{\perp}(t) = \frac{1}{3}I(t)[1 - r(t)] \tag{A2}$$

In these equations it is understood that $I(t)$ or $r(t)$ can be the result of one- or two-photon excitation. The phase angle difference ($\Delta\omega$) between the polarized components and the ratio ($\Lambda\omega$) of the modulated amplitude are given by

$$\Delta_{\omega} = \arctan\left(\frac{D_{\|}N_{\perp} - D_{\perp}N_{\|}}{N_{\|}N_{\perp} + D_{\|}D_{\perp}}\right) \tag{A3}$$

$$\Lambda_{\omega} = \sqrt{\frac{N_{\|}^2 + D_{\|}^2}{N_{\perp}^2 + D_{\perp}^2}} \tag{A4}$$

where sine (N) and cosine (D) transforms of the emission are evaluated from the relations

$$N_{\|} = \int_0^{\infty} I_{\|}(t)\sin(\omega t)dt = \frac{1}{3}(n_1 + 2n_2) \tag{A5}$$

$$N_{\perp} = \int_0^{\infty} I_{\perp}(t)\sin(\omega t)dt = \frac{1}{3}(n_1 - n_2) \tag{A6}$$

$$D_{\|} = \int_0^{\infty} I_{\|}(t)\cos(\omega t)dt = \frac{1}{3}(d_1 + 2d_2) \tag{A7}$$

$$D_{\perp} = \int_0^{\infty} I_{\perp}(t)\cos(\omega t)dt = \frac{1}{3}(d_1 - d_2) \tag{A8}$$

For a multiexponential intensity and anisotropy decay [Eqs. (4) and (6)], the terms needed to evaluate the transforms are given by

$$n_1 = \sum_{i=1}^{3} \frac{\alpha_i\omega}{\omega^2 + \Gamma_j^2} \tag{A9}$$

$$n_2 = \sum_{i=1}^{3}\sum_{j=1}^{3} \frac{r_0\alpha_i g_j\omega}{\omega^2 + H_{ij}^2} \tag{A10}$$

$$d_1 = \sum_{i=1}^{3} \frac{\alpha_i\Gamma_i}{\omega^2 + \Gamma_i^2} \tag{A11}$$

$$d_2 = \sum_{i=1}^{3}\sum_{j=1}^{3} \frac{r_0\alpha_i g_j H_{ij}}{\omega^2 + H_{ij}^2} \tag{A12}$$

where $\Gamma_i = \tau_i^{-1}$, and $H_{ij} = \tau_i^{-1} + \theta_j^{-1}$.

ACKNOWLEDGMENTS

This work was supported by National Science Foundation Grant DMB-8804931, with support for instrumentation from NIH Grants RR-07510 and RR-08119. The authors thank Dr. Badri Maliwal for his assistance with preparation of the lipid samples.

REFERENCES

1. L. Goodman and R. P. Rava (1984) *Acc. Chem. Res.* **17**, 250–257.
2. D. M. Friedrich and W. M. McClain (1980) *Annu. Rev. Phys. Chem.* **31**, 559–577.
3. D. M. Friedrich (1982) *J. Chem. Educ.* **3**, 472–481.
4. M. J. Wirth, A. Koskelo, and M. J. Sanders (1981) *Appl Spectrosc.* **35**, 14–21.
5. B. Hudson and B. Kohler (1974) *Annu. Rev. Phys. Chem.* **25**, 437–460.
6. R. R. Birge (1986) *Acc. Chem. Res.* **19**, 138–146.
7. M. B. Masthay, L. A. Findsen, B. M. Pierce, D. F. Bocian, J. S. Lindsey, and R. R. Birge (1986) *J. Chem. Phys.* **84**, 3901–3915.
8. B. E. Anderson, R. D. Jones, A. A. Rehms, P. Ilich, and P. R. Callis (1986) *Chem. Phys. Lett.* **125**, 106–112.
9. A. A. Rehms and P. R. Callis (1987) *Chem. Phys. Lett.* **140**, 83–89.
10. R. R. Birge (1983) in D. S. Klinger, (Ed.), *Ultrasensitive Laser Spectroscopy*, Academic Press, New York, pp. 109–174.
11. S. M. Kennedy and F. E. Lytle (1986) Anal. Chem. **58**, 2643–2647.
12. S.-P. Jiang, S.-H., K.-C. Ruan, L.-K. Hui, S.-H. Liu, Z. Z. Zhang, and Q. Li (1984) *Chem. Phys. Lett.* **104**, 109–111.
13. S.-P. Jiang (1989) *Prog. React. Kinet.* **15**, 77–92.
14. J. R. Lakowicz, I. Gryczynski, Z. Gryczynski, E. Danielsen, and M. J. Wirth (1992) *J. Phys. Chem.* **96**, 3000–3006.
15. W. Denk, J. H. Strickler, and W. W. Webb (1990) *Science* **248**, 73–36.
16. D. W. Piston, D. R. Sandison, and W. W. Webb (1992) *Proc. SPIE* **1640**, 379–388.
17. J. R. Lakowicz, I. Gryczynski, E. Danielsen, and J. K. Frisoli (1992) *Chem. Phys. Lett.* **194**, 282–287.
18. J. R. Lakowicz and I. Gryczynski (1992) *Biophys. Chem.* **45**, 1–6.
19. J. R. Lakowicz and I. Gryczynski (1992) *J. Fluoresc.* **2**, 117–121.
20. C. D. Stubbs and B. W. Williams (1992) in J. R. Lakowicz (Ed.) *Topics in Fluorescence Spectroscopy, Vol. 3*, Plenum Press, New York, pp. 231–271.
21. L. A. Chen, R. E. Dale, S. Roth, and L. Brand (1977) *J. Biol. Chem.* **252**, 2163–2169.
22. S. Kawato, K. Kinosita, Jr., and A. Ikegami (1977) *Biochemistry* **24**, 376–383.
23. F. Jahnig (1979) *Proc. Natl. Acad. Sci.* **76**, 6361–6365.
24. P. P. Feofilov (1969) *Optics Spectrosc.* **26**, 306–310.
25. Y. T. Mazurenko (1971) *Optics Spectrosc.* **28**, 413–415.
26. W. M. McClain (1972) *J. Chem. Phys.* **57**, 2264–2272.

27. T. W. Scott, K. S. Haber, and A. C. Albrecht (1983) *J. Chem. Phys.* **78**, 150–157.
28. J. R. Lakowicz, G. Laczko, and I. Gryczynski (1986) *Rev. Sci. Instrum.* **57**, 2499–2506.
29. G. Laczko, J. R. Lakowicz, I. Gryczynski, Z. Gryczynski, and H. Malak (1990) *Rev. Sci. Instrum.* **61**, 2331–2337.
30. J. R. Lakowicz, E. Gratton, G. Laczko, H. Cherek, and M. Limkeman (1984) *Biophys. J.* **46**, 463–477.
31. E. Gratton, J. R. Lakowicz, B. P. Maliwal, H. Cherek, G. Laczko, and M. Limkeman (1984) *Biophys. J.* **46**, 479–486.
32. J. R. Lakowicz, H. Cherek, and B. P. Maliwal (1985) *Biochemistry* **24**, 376–383.
33. B. P. Maliwal and J. R. Lakowicz (1986) *Biochim. Biophys. Acta* **873**, 161–172.
34. G. Weber (1977) *J. Chem. Phys.* **66**, 4081–4091.
35. J. R. Lakowicz, I. Gryczynski, and E. Danielsen (1992) *Chem. Phys. Lett.* **191**, 47–53.
36. B. S. Hudson and B. E. Kohler (1972) *Chem. Phys. Lett.* **14**, 299–304.
37. H. L.-B. Fang, R. J. Thrash, and G. E. Leroi (1978) *Chem. Phys. Lett.* **57**, 59–63.
38. J. Saltiel, D. F. Sears, Jr., Y.-P. Sun, and J.-O. Choi (1992) *J. Am. Chem. Soc.* **114**, 3607–3612.
39. F. Mulders, H. van Langen, G. van Ginkel, and Y. K. Levine (1986) *Biochim. Biophys. Acta* **859**, 209–218.
40. M. Straume and B. J. Litman (1987) *Biochemistry* **26**, 5113–5120.
41. G. Weber (1978) *Acta Phys. Pol.* **A54**, 859–865.
42. J. R. Lakowicz and F. G. Prendergast (1978) *Biophys. J.* **24**, 213–231.
43. M. L. Johnson and S. G. Frasier (1985) *Methods Enzymol.* **117**, 301–342.
44. M. Straume, S. G. Frasier-Cadoret, and M. L. Johnson (1991) in J. R. Lakowicz (Ed.), *Topics in Fluorescence Spectroscopy*, Vol. 2, Plenum Press, New York, pp. 177–240.
45. J. R. Lakowicz, M. L. Johnson, N. Joshi, I. Gryczynski, and G. Laczko (1986) *Chem. Phys. Lett.* **131**, 343.
46. J. R. Knutson, D. G. Walbridge, and L. Brand (1982) *Biochemistry* **21**, 4671–4679.
47. H. Szmacinski, R. Jayaweera, H. Cherek, and J. R. Lakowicz (1987) *Biophys. Chem.* **27**, 233–241.
48. I. Gryczynski, unpublished observation.